ARCHIVES OF ELECTRICAL ENGINEERING VOL. 61(2), pp. 199-210 (2012)

DOI 10.2478/v10171-012-0017-z

Influence of constructional turbo-generator end region design on end winding inductances

MICHAEL FREESE, STEFAN KULIG

TU Dortmund University, Chair of Electrical Drives and Mechatronics
Emil-Figge-Str. 70, 44227 Dortmund, Germany
e-mail: {michael.freese/stefan.kulig}@tu-dortmund.de

(Received: 29.11.2011, revised: 05.12.2011)

Abstract: The paper introduces a comprehensive investigation in end winding inductances of large two-pole turbo-generators. With the aid of an analytic-numeric approach, where Neumann's formula is applied, the influence of geometric characteristics of double-layer stator end windings with involute shape is analysed. This parameter study results in approximation formulas for the stator self and mutual inductances at strand level as well as for the common used end winding leakage inductance. In order to consider field affecting components as pressure plate, flux shield, rotor shaft and rotor retaining ring, finite elements models for two machines (250 MVA and 1150 MVA) are created and computed. The results are integrated in the developed approximation formulas. Finally the simulation results of machine 1 are compared to the data of two different measurements. All approaches introduced in this paper show good correlation. The high speed of the analytic-numeric calculation is combined with the accuracy and opportunity to consider field affecting components within the extensive finite element computation successfully.

Key words: turbo-generator, end winding inductances, end winding leakage inductance

1. Introduction

In the last twenty years, especially in the few recent years, research activities in the field of end winding inductances have increased considerably. The reason for this development are advancements of hardware and software components which increase the ability to solve three dimensional field problems.

The authors in [1] and [2] apply analytic-numeric approaches to determine the end winding leakage inductances of squirrel cage induction machines and of turbo generators, respectively. The results are validated by measurements. In [3] and [4] finite elements analyses are used to identify the inductances in the end region of induction and AC machines. The obtained results are compared to measured data as well.

In most general machine analyses the end winding field is considered as a leakage field categorically and so the end region inductances are represented by end winding leakage inductances. The real distribution of the inductances in self and mutual inductances is not considered. Instead of this a substitute inductance, the end winding leakage inductance L_σ^w is

added within models based on the equivalent circuits by Park or within two-dimensional circuit coupled transient finite elements models. One common computation formula for L_σ^w is [5]:

$$L_\sigma^w = 2 \cdot \mu_0 w^2 \frac{l_w}{p} \cdot \lambda_{ws} \,. \tag{1}$$

The number of turns in series per strand is represented by w, l_w is the mean length of an end winding coil, p equates the number of pole pairs, λ_{ws} describes the magnetic permeance of the end region flux while both machine ends are considered by the coefficient 2.

The paper at hand combines the advantages of a fast and flexible analytic-numeric end winding inductance calculation using Neumann's formula with the accuracy and opportunity to consider field affecting components of the finite elements method. The first method is used to identify the influence of geometric winding parameters. The second one allows for the determination of correction coefficients concerning the field affecting components as pressure plate, flux shield, rotor shaft or rotor retaining ring, which cannot be included in the analytic-numeric method. The investigation concentrates on large two-pole turbo-generators and finally results in approximation formulas for the end winding inductances. As an additional reference two differing measurements are done and discussed.

2. Analytic-numeric approach

The analytic-numeric approach for inductance calculation is based on the solution of Neumann's integrals. Because the basics are already mentioned in [6] and [7] in detail, the most important and additional aspects are explained here.

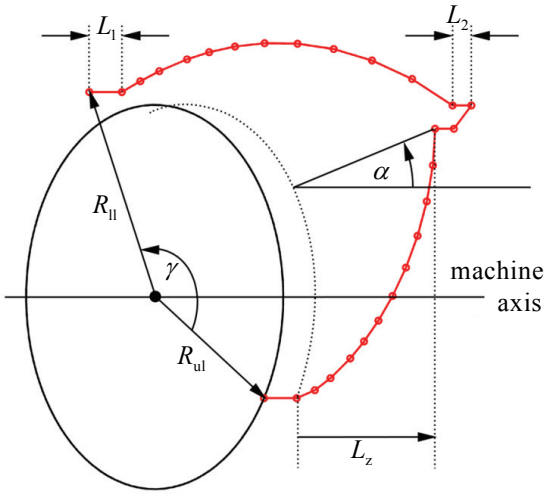

Fig. 1. Stator coil geometry in the end region with its characteristic parameters: radius R_{ll} (machine axis ↔ lower layer bar), radius R_{ul} (machine axis ↔ upper layer bar), coil span γ, conus angle α, straight section L_1, height of the connection piece L_2, outreach L_z

Neumann's integral has the following well-known form:

$$M_{vk} = \frac{\mu_0}{4\pi} \cdot \oint_{l_v} \oint_{l_k} \frac{\mathrm{d}\vec{l}_v \cdot \mathrm{d}\vec{l}_k}{r_{vk}} . \tag{2}$$

It provides the mutual inductance M_{vk} between two filamentary conductor loops v and k in air, where r_{vk} describes the distance between the two infinitesimal elements $\mathrm{d}l_v$ and $\mathrm{d}l_k$. The integral can be simplified by replacing the real conductor loop geometry as a connection of n_v resp. n_k short straight pieces of wire:

$$M_{vk} = \frac{\mu_0}{4\pi} \cdot \sum_{m_v=1}^{n_v} \sum_{m_k=1}^{n_k} \int_{l_{m_v}} \int_{l_{m_k}} \frac{\mathrm{d}\vec{l}_{m_v} \cdot \mathrm{d}\vec{l}_{m_k}}{r_{mvk}} . \tag{3}$$

The solutions for arbitrary located filamentary elements are provided in [8, 9].

In order to apply this method on turbo-generator end windings, coils with real cross-sections have to be modelled as filamentary coils. Within the scope of this work the inductance computation is implemented in MATLAB, which on the one hand allows for the direct input of the coordinates of an adequate number of cross section centres. On the other hand the stator end winding with its involute sections can be built up with the aid of involute functions analogue to [2]. A stator coil with its characteristic geometric parameters is shown in Figure 1. In the case of a symmetric stator winding the knowledge of only one coil geometry and of the number of coils is sufficient to create the whole stator winding. However, the rotor winding has a simple cylindrical shape, which is characterized by straight and arched sections.

As Neumann's formula can only be applied to conductor loops in air, the influence of magnetic and conductive components cannot be considered directly. However, there is the possibility to use the method of images to take the influence of the front end of the machine into account approximately. Here the two limiting cases are assumed as shown in Figure 2.

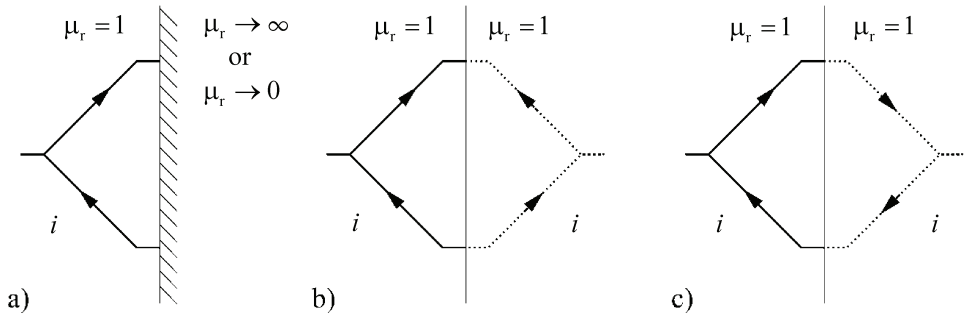

Fig. 2. a) current flow conductor loop in front of an infinite wide half-space, b) alternative configuration for $\mu_r \to \infty$, c) alternative configuration for $\mu_r \to 0$

The first one is characterized by the assumption of perpendicular $(\mu_r \to \infty)$, the second one by the assumption of parallel $(\mu_r \to 0)$ flux at the front end. Applying the method of

images results in a configuration of real and virtual conductors in air which finally allows the use of Neumann's formula. Indeed there are circuits discussed, which do not comply with the Kirchhoff's circuit law. But the identification of end winding inductances itself is done for unclosed circuits and affords only partial inductances of one coil or strand, so this approach is valid anyway.

The analytic-numeric approach can be applied on every single coil in the end region and thus provides an inductance matrix at coil level. This matrix can be used directly for the calculation of asymmetric conditions in the machine like inner faults cause (e.g. phase-to-phase or turn-to-turn faults). Considering the connection of single coils concerning coil groups and strands, the inductance matrix can be reduced stepwise as already described in [6].

3. Finite elements analysis

In order to identify the influence of magnetic and conductive components in the end region on the inductances two machine models are analysed with FLUX 3D using the finite elements method. The machines differ in power and end winding architecture. One of these models (machine 2) is shown in Figure 3. It consists of pressure plate, flux shield, rotor shaft and rotor retaining ring and is overlaid with filamentary stator and rotor coils. The laminated flux shield is used to avoid a penetration of the end region field into the stator core by channelising the flux. At Machine 1 such a component is missing. Here the eddy currents within the pressure plate have a shielding effect as well, but they cause ohmic losses additionally.

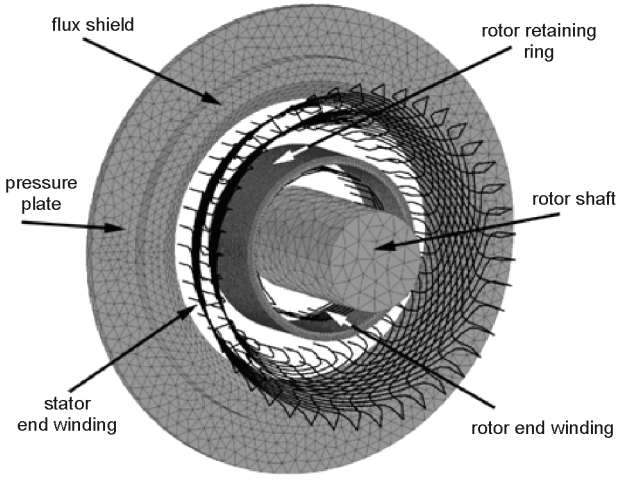

Fig. 3. End region model (machine 2) in FLUX 3D® as a superposition of finite elements model and winding model (stator and rotor winding)

At rated operating conditions the rotor rotates with the stator rotary field synchronously, so eddy currents within the non-magnetic, but conductive rotor retaining ring occur only marginally. Therefore the rotor retaining ring can be neglected in this case. For transients this

neglect is not valid anymore, because in this case eddy currents do occur in the retaining ring and damp the end region field. In order to calculate eddy currents properly a suitable fine mesh has to be generated. The mesh size depends on the depth of penetration δ with

$$\delta = \sqrt{\frac{1}{\pi \cdot f \cdot \mu \cdot \gamma}}, \tag{4}$$

where are f rated frequency, μ permeability and γ conductivity of the eddy current carrying component. The mesh size should not exceed the half penetration depth. While the penetration depth of a non-magnetic ($\mu = \mu_0$) rotor retaining ring is comparatively large, it is very small regarding a magnetic (e.g. $\mu = 1000 \cdot \mu_0$) and conductive pressure plate. Here the required mesh width may be much less than 1 mm. Because the pressure plate is a huge component of the end region model an adequate mesh needs a lot of memory for the multiplicity of elements, which only high end computers provide. In order to avoid such hardware problems an alternative approach in FLUX 3D can be chosen. The software features the possibility to use the *surface impedance formulations* [10]. The main advantage of this method is that only the surfaces of the eddy current carrying volumes have to be meshed, so that less main memory is required. The size of the face elements can be increased in this way as well. The applied method demands a sensible treatment of the single components as well as an accurate and valid choice of field formulations. Figure 4 shows an overview concerning the considered end region components of machine 1 and their treatment in FLUX 3D.

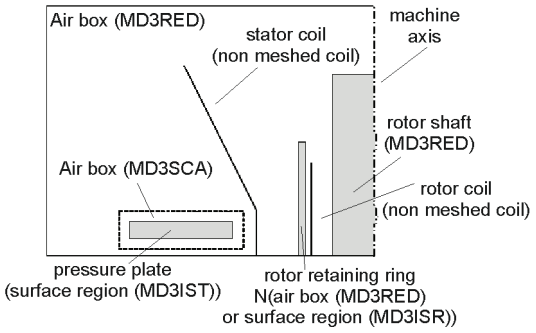

Fig. 4. Principal drawing of the considered end region components (machine 1) and their treatment within the finite elements computation in FLUX 3D; for the description of the formulations see [10]

The inductance computation is done successively for all stator and rotor coils, where eddy currents are considered if necessary. For rating only the eddy-currents in the pressure plate of machine 1 are taken into account within a harmonic calculation. However, computing machine 2 with its laminated flux shield there is no need to regard any eddy-currents. In contrast eddy currents do occur in the rotor retaining ring during transients for both machines. In order to get a rough impression of their effects on the end winding inductances a configuration is chosen and analysed where one stator coil is fed by a sinusoidal current and the rotor retaining ring is considered as a stagnant conductive component.

4. Measurements

Besides the aforementioned approaches to identify the end winding inductances by simulations, measurements are taken of machine 1 to get an additional possibility of comparison. Two different measurements are applied and explained in the following. They have in common that they are done at a machine with missing rotor.

The first measurement is based on a single phase excitation of the stator winding according to Figure 5 and allows for the determination of the self and mutual inductances of the stator strands by measuring the voltage in the fed strand and the induced voltages in the opened strands.

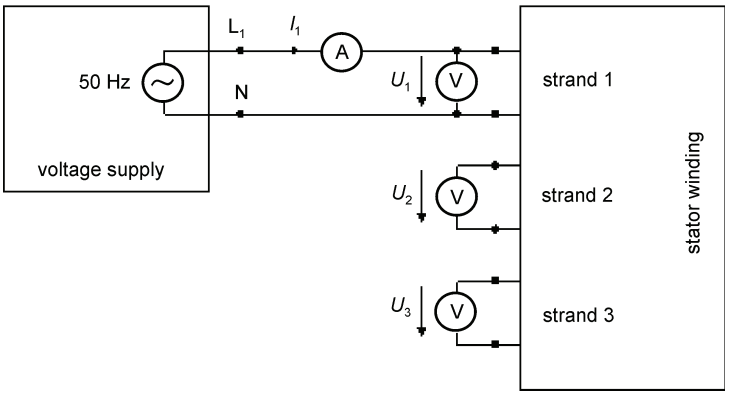

Fig. 5. Setup measurement 1

The inductances can be calculated as

$$M_{i1} = M_{1i} = \frac{U_i}{\omega I_1} \quad (\text{here: } i = 1 \ldots 3) \tag{5}$$

and result in an experimentally (index e) determined inductance matrix $\boldsymbol{M}_{\mathrm{str}}^{\mathrm{e}}$ at strand level (index str):

$$\boldsymbol{M}_{\mathrm{str}}^{\mathrm{e}} = \begin{bmatrix} M_{11}^{\mathrm{e}} & M_{12}^{\mathrm{e}} & M_{13}^{\mathrm{e}} \\ M_{21}^{\mathrm{e}} & M_{22}^{\mathrm{e}} & M_{23}^{\mathrm{e}} \\ M_{31}^{\mathrm{e}} & M_{32}^{\mathrm{e}} & M_{33}^{\mathrm{e}} \end{bmatrix}. \tag{6}$$

In addition to the measurement a two-dimensional finite elements calculation is done to identify the inductance matrix $\boldsymbol{M}_{\mathrm{str}}^{\mathrm{a}}$ for the active part (index a) of the machine, which has the same structure as $\boldsymbol{M}_{\mathrm{str}}^{\mathrm{e}}$. Finally the end winding (index w) inductance matrix $\boldsymbol{M}_{\mathrm{str}}^{\mathrm{w}}$ can be calculated as

$$\boldsymbol{M}_{\mathrm{str}}^{\mathrm{w}} = \boldsymbol{M}_{\mathrm{str}}^{\mathrm{e}} - \boldsymbol{M}_{\mathrm{str}}^{\mathrm{a}}. \tag{7}$$

According to the standard IEC 60034-4:2008, the second measurement is based on a three phase excitation of the stator winding and allows for the determination of the so called leakage inductance of the stator winding. While the stator winding is supplied with a symmetric three-phase system, an exploring coil is positioned within the bore which catches the flux through the bore. The measurement setup is shown in Figure 6.

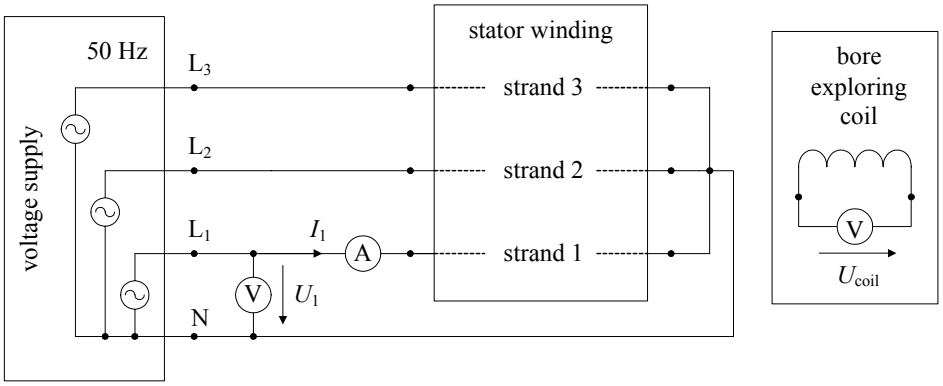

Fig. 6. Setup measurement 2

The exploring coil span complies with the pole pitch, so for a two-pole machine it complies with a diameter coil. On the one hand the measurement affords the three-phase strand inductance L_1^{e} with

$$L_1^{\mathrm{e}} = \frac{U_1}{\omega I_1}. \tag{8}$$

On the other hand measuring the induced voltage in the bore exploring coil leads to the bore inductance $L_{\mathrm{b}}^{\mathrm{e}}$ (relating to the stator)

$$L_{\mathrm{b}}^{\mathrm{e}} = \frac{U_{\mathrm{coil}}}{\omega I_1} \cdot \frac{N_1 \xi_1}{N_{\mathrm{coil}} \xi_{\mathrm{coil}}}, \tag{9}$$

where the coefficient $N_1\xi_1 / N_{\mathrm{coil}}\xi_{\mathrm{coil}}$ considers the effective numbers of turns.

The two identified inductances can be used to determine the leakage inductance L_σ^{e} of the whole machine (without rotor):

$$L_\sigma^{\mathrm{e}} = L_1^{\mathrm{e}} - L_{\mathrm{b}}^{\mathrm{e}}. \tag{10}$$

A two-dimensional numeric field calculation for the active component of the machine complements the results from the measurement where the same values are determined in principal. Only the end winding cannot be considered in the 2D finite elements calculation. However, the end winding leakage inductance can be computed nevertheless by

$$L_\sigma^{\mathrm{w}} = L_\sigma^{\mathrm{e}} - L_\sigma^{\mathrm{a}}. \tag{11}$$

5. Results

At first the analytic-numeric calculation results are compared to those evaluated with the finite elements method. The comparison is done neglecting all field affecting components in the end region and assuming parallel flux at the front end. The computed inductances show very good analogy as Figure 7 verifies for the self and mutual inductances of one stator coil referring to itself and to the other 65 stator coils.

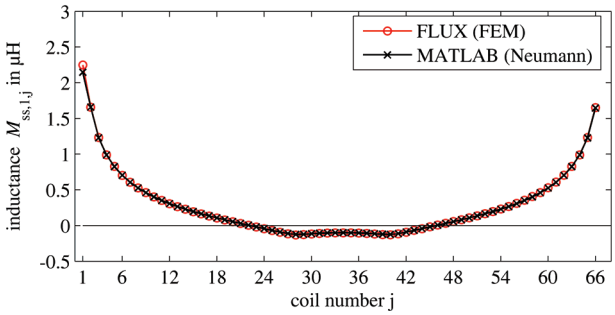

Fig. 7. Comparison of the stator inductances at coil level determined by the finite elements method (FEM) and by the analytic-numeric approach using Neumann's formula

The transformation of the inductances from coil level to strand level results in two inductance matrices $\boldsymbol{M}^{\mathrm{w}}_{\mathrm{str,\,Flux}}$ and $\boldsymbol{M}^{\mathrm{w}}_{\mathrm{str,\,Matlab}}$ for both approaches according to Table 1. The deviation of the entries does not exceed 1% which is negligible small.

Table 1. Reduced inductance matrices of the end winding at strand level computed with FLUX 3D and MATLAB

$\boldsymbol{M}^{\mathrm{w}}_{\mathrm{str,\,Flux}}$ in µH			
144	−45	−45	$778 \cdot \sin(\varphi)$
−45	144	−45	$778 \cdot \sin(\varphi + 120°)$
−45	−45	144	$778 \cdot \sin(\varphi - 120°)$
$778 \cdot \sin(\varphi)$	$778 \cdot \sin(\varphi + 120°)$	$778 \cdot \sin(\varphi - 120°)$	31970

$\boldsymbol{M}^{\mathrm{w}}_{\mathrm{str,\,Matlab}}$ in μH			
143	−45	−45	$771 \cdot \sin(\varphi)$
−45	143	−45	$771 \cdot \sin(\varphi + 120°)$
−45	−45	143	$771 \cdot \sin(\varphi - 120°)$
$771 \cdot \sin(\varphi)$	$771 \cdot \sin(\varphi + 120°)$	$771 \cdot \sin(\varphi - 120°)$	31872

In order to identify the influence of magnetic and conductive components in the end region the finite elements models are expanded by these parts, which are: pressure plate (DP), flux

shield (STSR), rotor retaining ring (LK) and rotor shaft (RW). Because of the symmetric structure of $\boldsymbol{M}_{\mathrm{str}}^{\mathrm{w}}$ only the quantities marked in grey M_{11}^{w}, M_{21}^{w} and M_{41}^{w}, the associated reactances X_{11}^{w}, X_{21}^{w}, and X_{41}^{w}, respectively, and additionally the leakage reactance X_{σ}^{w} are mentioned in the following.

All these quantities (in p.u.) are listed in Table 2 and Table 3 depending on the considered components. Concerning machine 1 the results obtained through measurements and 2D field calculations are listed as well.

Table 2. Selective reactances of the end windings of machine 1

Machine 1 (250 MVA)	X_{11}^{w} / p.u.	X_{21}^{w} / p.u.	X_{41}^{w} / p.u.	X_{σ}^{w} / p.u.
–	0.0456	– 0.0142	$0.246\cdot\sin(\varphi)$	0.0598
DP	0.0519	– 0.0174	$0.290\cdot\sin(\varphi)$	0.0693
DP, RW	0.0579	– 0.0203	$0.455\cdot\sin(\varphi)$	0.0782
DP, RW, LK	0.0456	– 0.0146	$0.218\cdot\sin(\varphi)$	0.0602
DP (meas. & simul., 1-phase)	0.0725	– 0.0241	–	0.0966
DP (meas. & simul., 3-phase)	–	–	–	0.0997

Table 3. Selective reactances of the end windings of machine 2

Machine 2 (1150 MVA)	X_{11}^{w} / p.u.	X_{21}^{w} / p.u.	X_{41}^{w} / p.u.	X_{σ}^{w} / p.u.
–	0.0362	– 0.0119	$0.082\cdot\sin(\varphi)$	0.0481
DP, STSR	0.0506	– 0.0183	$0.124\cdot\sin(\varphi)$	0.0689
DP, STSR, RW	0.0570	– 0.0218	$0.191\cdot\sin(\varphi)$	0.0788
DP, STSR, RW, LK	0.0411	– 0.0149	$0.063\cdot\sin(\varphi)$	0.0560

It is obvious, that both the pressure plate and the rotor shaft have a considerable influence on the end winding inductances. Also and especially the flux shield causes comparatively high inductances. However, eddy currents within the rotor retaining ring during disturbances decrease the inductances (see Fig. 8). Regarding the results for machine 1 this case corresponds to the configuration, where neither pressure plate, rotor shaft nor rotor retaining ring are present. At this point it should be mentioned again, that in case of faulty operating conditions the results allow only a rough classification of the conditions in the machine.

The comparison between the simulated inductances with the inductances determined by the measurements in combination with 2D field calculation shows a deviation of about 30%. The reason for this relative high deviation can be found in the 2D field calculation. Because the inductances of the active machine part are much higher than the end winding inductances, small changes of the 2D simulation results of about 5 to 12% (in the present cases) can reduce the deviation to only a few per cent. In addition to this the two end regions have not exactly the same geometry due to the fact that the coils on one side (CE) have to be connected to each

other and to the power supply. Thus the comparison between measurements and simulations shows adequate accordance nevertheless.

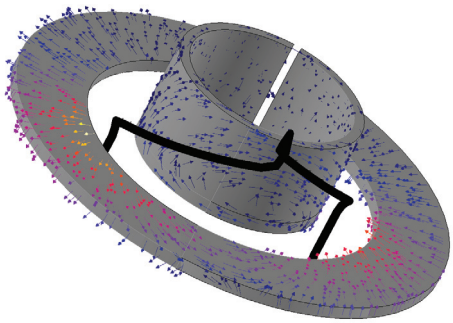

Fig. 8. Visualisation of the eddy currents in pressure plate and rotor retaining ring of machine 1 caused by sinusoidal excitation of a stator coil; cut through the two components necessary due to constraints of surface impedance condition in the context of hollow conductors

In addition to the identification of the influence of magnetic and conductive components in the end region a parameter study is done. The aim of this study is to clarify which of the geometric quantities according to Figure 1 have a significant influence on the end winding inductances. The study is applied concerning X_{11}^{w}, X_{21}^{w} and X_{σ}^{w} and considers typical values for the turbo generator parameters. It shows that L_2 and α can be neglected for the machine type under investigation. The parameters L_z, R_{ul}, L_1 and the arc $L_3 = \gamma \cdot \pi / 180° \cdot R_{\mathrm{ul}} = Y \cdot \pi \cdot R_{\mathrm{ul}}$ (all given in meters) have almost linear characteristics, so the inductances (in Henry) can be approximated with the aid of linear approaches:

$$M_{11}^{w} = 2 \cdot 10^{-2} \cdot \mu_0 \cdot \left(\frac{2 \cdot w}{a}\right)^2 \cdot \left(-1.5\ \mathrm{m} + 55 \cdot L_1 + 22 \cdot L_z + (31 \cdot \pi \cdot Y - 44) \cdot R_{\mathrm{ul}}\right) \cdot c_{11}, \quad (12)$$

$$M_{21}^{w} = 2 \cdot 10^{-2} \cdot \mu_0 \cdot \left(\frac{2 \cdot w}{a}\right)^2 \cdot \left(23 \cdot L_1 + 6 \cdot L_z + (9 \cdot \pi \cdot Y - 13) \cdot R_{\mathrm{ul}}\right) \cdot c_{21}, \quad (13)$$

$$M_{\sigma}^{w} = 2 \cdot 10^{-2} \cdot \mu_0 \cdot \left(\frac{2 \cdot w}{a}\right)^2 \cdot \left(-1.5\ \mathrm{m} + 78 \cdot L_1 + 28 \cdot L_z + (40 \cdot \pi \cdot Y - 57) \cdot R_{\mathrm{ul}}\right) \cdot c_{\sigma}, \quad (14)$$

Besides the aforementioned parameters the formulas contain the coefficient 2 to consider both machine ends, the vacuum permeability μ_0 and a quadratic coefficient, which is the square of the number of turns of one strand and which consists of the number of turns of a coil group w and the number of parallel ways per strand a. Furthermore a correction coefficient c considers the influence of the field affecting components in the end region. Before this coefficient is discussed the accuracy of (14) is shown and compared to that of the approximation formula (1) mentioned within the introduction, where λ_{w} is set to 0.4 as recommended in [5] for involute double layer windings. The basis of comparison are the values received by the calculation program in MATLAB.

If the correction coefficient c_{σ} is set to 1 (which means no field affecting components are considered), the accuracy of (14) is almost zero for most of the 900 different parameter sets as

Figure 9 demonstrates. However, the leakage inductance calculation according to (1) shows, that using only the mean length of an end winding coil is not as accurate.

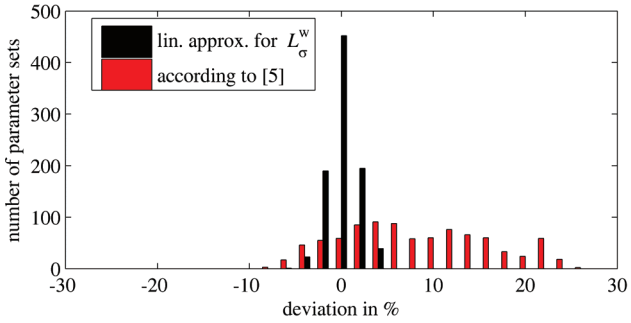

Fig. 9. Percentaged deviation of the end winding inductances of 900 parameter sets referring to the inductances computed with Neumann's Formula in MATLAB

Finally the correction coefficients c_{11}, c_{21} and c_σ are identified concerning the two machines under investigation by the finite elements computation. They are listed in Table 4.

Table 4. Correction coefficients to consider the field affecting end region components

	Machine 1		Machine 2	
	without LK	with LK	without LK	with LK
c_{11}	1.27	1.00	1.57	1.14
c_{21}	1.14	1.03	1.83	1.25
c_σ	1.31	1.01	1.64	1.16

6. Conclusion

The investigation on end winding inductances of large two-pole turbo-generators with involute stator coil shape provides approximation formulas for the self and mutual inductances as well as for the end winding leakage inductance of the stator strands. These formulas are based on a comprehensive geometric parameter study, which is done with a fast end winding inductance calculation program developed in MATLAB. Because of the impossibility to consider all magnetic and conductive components in this program, finite elements models for two machines with differing end region architecture are created and computed in FLUX 3D. Before analysing the particular influences, a comparison between the two approaches is done which shows very good correlation. Finally the identified influences of the field affecting components on the end winding inductances are integrated in the developed approximation formulas through correction factors. The analysis shows, that especially the presence of a flux shield enlarges the end winding inductances. But also pressure plate and rotor shaft have an

influence on the end winding inductances. Eddy currents in the rotor retaining ring during transients damp the end region field and thus the end winding inductances as well.

Acknowledgement
The authors thank the Deutsche Forschungsgemeinschaft (DFG/German Research Foundation) for the financial support which allowed for the comprehensive investigation. Furthermore, they are grateful to SIEMENS Erfurt for the possibility to take measurements.

References

[1] Dornau U., *Berechnung und Messung der Stirnstreuung von Asynchronmaschinen mit Käfigläufer.* Dissertation at the chair of Theoretical Electrical Engineering and Electrical Machines (today Electrical Drives and Mechatronics), TU Dortmund University (1990).
[2] Ban D., Zarko D., Mandic I., *Turbogenerator End winding Leakage Inductance Calculation Using a 3-D Analytical Approach Based on the Solution of Neumann Integrals*. IEEE Transactions on Energy Conversion 20(1), (2005).
[3] Brahimi A.T., Foggia A., Meunier G., *End Winding Reactance Computation Using a 3D Finite Element Program*. IEEE Transactions on Magnetics 29(2), (1993).
[4] Chiver O. et al., *About End Winding Inductance Computation of AC Machines Using FEM 3D.* International Conference of the Carpathian Euro-Region Specialists in Industrial Systems, 7th Edition (2008).
[5] Müller G., Vogt K., Ponick B., *Berechnung elektrischer Maschinen* (*Computation of Electrical Machines,* in German). Wiley-VCH Verlag GmbH & Co. KGaA, 6th Edition (2008).
[6] Freese M., *Analytic Calculation of Turbo Generator End Winding Inductances using Neumann's Formula*. International Symposium on Power Electronics, Electrical Drives, Automation and Motion (SPEEDAM), Pisa, Italy (2010).
[7] Freese M., *Comparison between an Analytic Method and a Numerical Calculation to Determine the End Winding Inductances of a Turbo Generator*. International Conference on Electrical Machines (ICEM), Rom, Italy (2010).
[8] Hannakam L., Nolle E., *Program for Determination of Mutual Inductances of spatial polygon-shaped conductor loops* (in German). Archiv für Elektrotechnik 64: 21-25 (1981).
[9] Sommer K., *Development of a Program for the Determination of Mutual Inductances of filamentary conductor loops, which course is straight in sections, using Neumann's formula* (in German). Research paper at the chair of Theoretical Electrical Engineering and Electrical Machines (today Electrical Drives and Mechatronics), TU Dortmund University (1989).
[10] Cedrat, Physical Applications. FLUX® 9.10 3D Application, User's Guide, 5 (2005).